International Research Journal of Engineering and Technology (IRJET) e-ISSN: 2395-0056
Volume: 10 Issue: 06 | Jun 2023 www.irjet.net p-ISSN: 2395-0072

Comparison of Performance for Power Quality Improved EV Battery Chargers using Bridgeless Cuk Converter and SEPIC PFC Converter

Namburi Ramya Sri

(M. Tech, Department of Electrical Engineering, JNTUH University College of Engineering, Science and Technology Hyderabad, India)

Abstract- This paper compares the performance of two power factor correction (PFC) converters, the bridgeless Cuk converter and the SEPIC PFC converter, in improving power quality for electric vehicle (EV) battery chargers. The converters are evaluated based on power factor, total harmonic distortion (THD) and efficiency. Simulations using an EV battery charging system demonstrate the converters effectiveness in reducing THD, improving power factor, achieving high efficiency, and maintaining stable output voltage. The findings aid in selecting and designing efficient and reliable EV charging systems, contributing to grid stability. Furthermore, this research lays the groundwork for future advancements in power electronics for EV charging applications.

Keywords: Electric vehicle battery chargers, power factor correction, bridgeless Cuk converter, SEPIC PFC converter, power quality improvement, total harmonic distortion (THD), efficiency, voltage regulation

1.INTRODUCTION

Traditional electric vehicle (EV) battery chargers encounter issues with power quality and efficiency due to the non-linear behavior of the input diode bridge rectifier used in the AC-DC conversion stage. These chargers draw irregular current from the mains, leading to a deteriorated power factor and high total harmonic distortion of up to 55.3% [1]. To comply with international standards like the IEC 6100-3-2 [2] and enhance input power quality, power factor correction converters (PFC) are replacing the conventional chargers at AC-DC conversion stage.

The efficiency of DBR-fed chargers is hampered by conduction loss resulting from the input diodes. Bridgeless PFC converters offer a viable solution by reducing conduction loss and enhancing power quality in EV chargers. Several improved power quality converters have been examined in [3]. The utilization of buck and boost converters [4] in EV chargers for power factor correction (PFC) is unsuitable due to their limitations in current shaping and duty cycle. The bridgeless buck-boost converter [5] presents an attractive solution for PFC in EV chargers as it allows a wide range of duty cycle variation to control the output voltage.

Cuk and SEPIC converters have been analyzed in [6]. The Cuk converter exhibits favorable charging characteristics with low ripple in battery current, unlike the SEPIC converter, which has the limitation of discontinuous output current. The bridgeless Cuk converter [7] provides advantages such as lower input current, reduced EMI, and straight forward implementation. However, it also has drawbacks like a floating neutral, floating terminal for the load, and circulating losses. Current shaping is achieved using average current mode control and voltage follower mode control. The converter's operation mode, either CCM or DCM, determines the PWM switching strategy.

In order to achieve an affordable charging solution, the converter operates in DCM (Discontinuous Conduction Mode) with PWM (Pulse Width Modulation) control based on voltage feedback. By implementing this approach, cost-effectiveness can be achieved in the charging process. Variable duty cycle control-based PWM switching is employed for its excellent current shaping capability [8]. A flyback converter is also designed to operate in DCM mode [9], featuring a cascaded dual-loop controller for regulating battery charging in CC and CV charging regions. In accordance with SAE standard J1772 [10], EV battery chargers should be lightweight, efficient, cost-effective, and provide low ripple charging.

To fulfil these requirements, a research work Comparison of Performance for Power Quality Improved EV Battery Chargers using Bridgeless Cuk Converter and SEPIC PFC Converter is proposed which involves the design and development of a bridgeless Cuk converter, a Flyback converter with a control unit, and SEPIC (Single-Ended Primary Inductance Converter) a Flyback converter with a control unit. These designs are implemented using Simulink to ensure optimal power factor correction (PFC) characteristics. A comparative analysis is performed to evaluate the effectiveness of these two solutions for EV battery chargers. The charger offers simplified control, reduced size and cost, improved efficiency, elimination of circulating losses, and reduced electromagnetic interference. The control of the PFC converter is simplified by employing the same gate drive and control circuitry for each half cycle.

In this paper, the design of the output inductors for the Cuk converter is optimized specifically for Discontinuous Conduction Mode (DCM), resulting in a reduction in both the

cost and size of the converter. Compared to other designs, the Bridgeless Cuk converter significantly minimizes the number of components involved within one switching cycle, leading to enhanced efficiency of the charger. The operation of the intermediate capacitors independently in both halves of the converter eliminates any circulating losses.

The implementation of a common ground arrangement for the two switches in the proposed topology contributes to a decrease in electromagnetic interference. The DC link voltage of the Cuk converter is regulated at a controlled level of 400V. To validate the effectiveness of the proposed EV charger, a simulation model has been developed and demonstrates improved performance in steady-state conditions, while charging a 48V, 100Ah lead-acid battery for electric vehicles (EVs).

2. CONFIGURATION, OPERATING PRINCIPLE, DESIGN OF BRIDGELESS CUK CONVERTER BASED EV BATTERY CHARGER

A. Configuration of Bridgeless Cuk Converter Based EV Battery Charger

Figure 1 illustrates the recommended configuration of an advanced EV charger, comprising a flyback converter and a bridgeless (BL) Cuk power factor correction (PFC) converter. The suggested PFC Cuk converter operates with components including output diode Do1, switch S1, input inductor Li1, and output inductor Lo1 for the positive half-cycle. Similarly, during the subsequent half cycle, switch S2, input inductor Li2, output diode Do2, and inductor Lo2 are utilized. The PFC Cuk converter maintains a constant DC link voltage through the use of a single voltage sensor and single-loop voltage feedback control.

A cascaded dual loop controller is employed in the flyback converter to regulate the battery current during the charging process in both constant current (CC) and constant voltage (CV) regions.

B. Operating Principle of Bridgeless Cuk Converter Based EV Battery Charger

This section outlines the fundamental operation of the proposed EV charger. Due to waveform symmetry, only the positive half cycle of the BL converter is considered in Figures 2 (a)-(c).

1. Operation of BL Cuk PFC Converter

   At time t1, the gate pulse applied to switch S1 initiates the first mode of operation (P-I) for the positive half cycle, resulting in a linear increase in the current flowing through input inductor Li1 as depicted in Figure 3. Capacitor C1 begins discharging through switch S1 and output inductor Lo1, as shown in Figure 2(a).

   At time t2, when the gate pulses to the switch are turned off, mode P-II begins as the polarity of capacitor C1 reverses. Figure 2(b) illustrates the discharge of stored energy from input inductor Li1 through converter capacitor C1 and diode Do1. The discharge of the output inductor occurs through the output diode and the DC connection capacitor Ccuk. Mode P-III starts at time t3 when the output inductor Lo1 is fully drained, as shown in Figure 2(c), and the current through the output inductor drops to zero. The flyback converter connected to the output of the PFC Cuk Converter receives the required power from the DC-link capacitor Ccuk as the Cuk Converter operates in DCM mode at this point.

2. Operation of Flyback Converter

   The flyback converter's operation is examined based on the discontinuous conduction mode (DCM) of the magnetizing inductance in the high-frequency transformer (HFT). The current flowing through the magnetizing inductance Lmf increases steadily, storing energy when the flyback switch Sf is turned on. At this moment, the dot convention of the HFT causes the output diode Df to be reverse biased. During the switch-off phase, when the polarity of the HFT is reversed, the output power is transferred to the battery as the output diode Df becomes forward biased. However, during each switching cycle, when the magnetizing inductance is fully discharged, the required battery charging current in constant current (CC) mode is supplied by the output capacitor Cbatt.

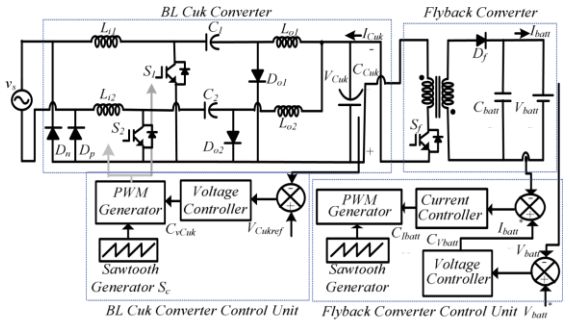

Fig.1. Circuit diagram of Bridgeless Cuk Converter based EV battery Charger

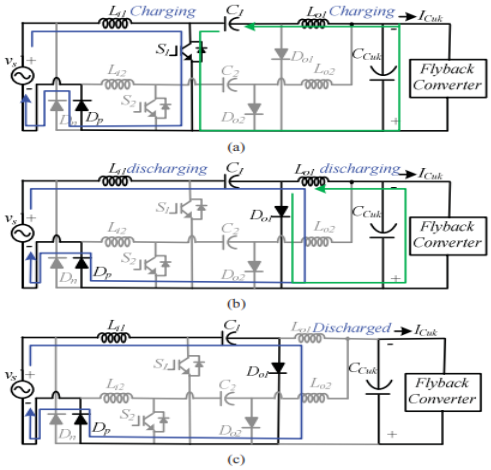

Fig.2.The operation of the BL PFC Cuk Converter fed EV Charger circuit (a)Mode P-I, (b)Mode P-II, and (c)Mode P-III.

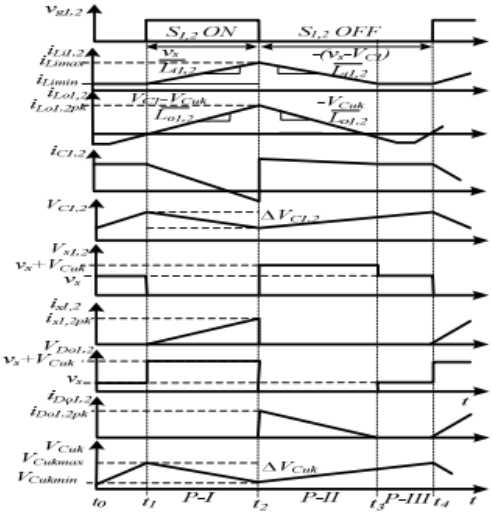

Fig.3.Associated switching behavior of the different components over one switching cycle.

C. Design of Bridgeless Cuk Converter Based EV Battery Charger

Based on the given design expressions in [11], an electric vehicle (EV) charger is created by combining a bridgeless Cuk converter and a flyback converter operating in DCM. The symbols and constants used in the calculations correspond to the values depicted in Figure 1.

3. OPERATING PRINCIPLE AND DESIGN OF SEPIC PFC CONVERTER BASED EV BATTERY CHARGER

A. Operating Principle of SEPIC PFC Converter based EV battery Charger

As seen in Fig.4, the enhanced SEPIC converter-based EV charger A PFC converter is used at the front end of the charger to give better PQ characteristics, and an isolated converter is used to regulate the charging current flowing through the electric vehicle battery. With a high voltage gain, the output of this PFC converter is kept constant at 300V. When compared to a continuous conduction mode (CCM)-based design in the PFC circuit, the DCM design for this converter uses fewer sensors. In turn, this lowers the converter's price and control complexity. The suggested converter is an altered version of a standard SEPIC converter with a few auxiliary component's version of a standard SEPIC converter with a few auxiliary components added to raise the voltage gain above that of existing non-isolated SEPIC converters.

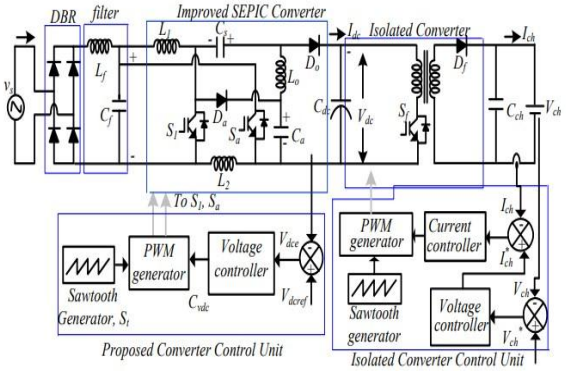

Fig.4. Circuit diagram of SEPIC PFC Converter based EV battery Charger

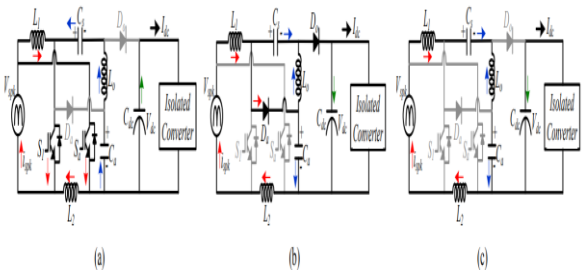

Fig.5.Operating principle of the enhanced SEPIC PFC (Power Factor Correction) converter. It showcases three modes: Mode I, Mode II, and Mode III.

1. Operation of SEPIC Converter

The primary switch S1, input inductor L1, output inductor Lo, intermediate capacitor Cs, and output diode Do make up this PFC converter. The auxiliary switch Sa, input inductor L2, intermediate capacitor Ca, and diode Da make up the PFC converter. The operation of the converter is described in the following manner, assuming that the output inductor of this SEPIC converter is set to function in DCM for one switching cycle Ts. (t1-t2) Mode-I: In this configuration, the instant t1 results in the

activation of the auxiliary switch Sa as well as the main switch S1. As seen in Fig. 5 (a), the output diodes Do and Da are reverse-biased.

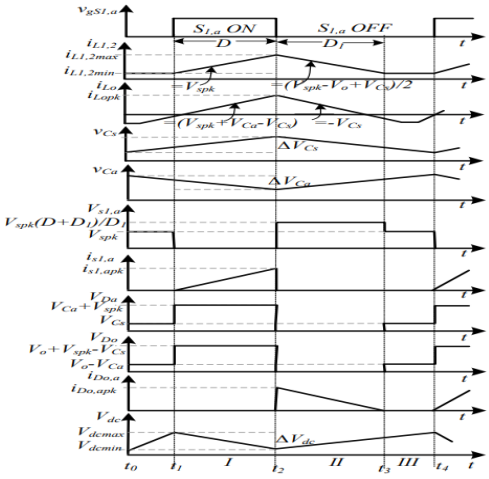

Fig.6.Waveforms of SEPIC PFC converter over single switching cycle

According to Fig.6, the currents flowing through the two input inductors (iL1, iL2) and the output inductor current (iLo), which are written as follows, rise linearly with a slope proportional to the input voltage Vspk.

$$\frac{di_{L1}}{dt} = \frac{di_{L2}}{dt} = \frac{V_{spk}}{L_1 (=L_2)}$$

$$\frac{di_{Lo}}{dt} = \frac{V_{spk}}{L_o} \qquad (1), (2)$$

As soon as the pulses turn S1 and Sa off, Mode-II (t2-t3) begins. Do and Da, the output and auxiliary diodes, begin to conduct. Through the auxiliary diode Da, the input inductors L1 and L2 send the stored energy to the isolated converter. As seen in Fig.5(b), the output inductor Lo dissipates its energy through the diode Do. The three inductor currents' expressions are written as,

$$\frac{di_{L1}}{dt} = \frac{di_{L2}}{dt} = \frac{V_{spk} - V_{dc} + V_{C_s}}{2L_1 (= L_2)}$$

$$\frac{di_{Lo}}{dt} = -\frac{V_{C_S}}{L_o} \qquad (3),(4)$$

The voltages across the DC-link capacitor, Cdc, and series capacitor Cs are shown in Fig.6 as Vdc and Vcs. Mode-III(t3-t4) Switches and diodes in the circuit are in a non-conducting state during this mode, which is also known as a discontinuous conduction mode. As seen in Fig. 5(c), the currents flowing through the output diode do decrease until they reach zero. Applying KVL in this mode to the loop formed by Vspk, L1, Cs, Lo, Ca, and L2 results in

$$-V_{spk} + v_{L1} - V_{C_s} - v_{Lo} + V_{C_a} + v_{L2} = 0 \quad (5)$$

where Vca, as depicted in Fig.6, is the voltage of the auxiliary capacitor. If the average voltage across the input inductors is set to zero, it produces

$$V_{spk} = V_{C_a} - V_{C_s} \qquad (6)$$

Similar to this, by using the volt-second equation to describe the proposed converter's input and output inductors throughout the duty cycle D, the following relationships are generated:

$$\frac{1}{T_s}\left(\int_0^{DT_s} V_{spk}\,dt + \int_{DT_s}^{T_s} \frac{\left(V_{spk} - V_{dc} + V_{C_s}\right)}{2} dt\right) = 0$$

$$\frac{1}{T_s}\left(\int_0^{DT_s} (V_{spk} + V_{C_a} - V_{C_s})dt \int_{DT_s}^{T_s} (-V_{C_s})dt\right) = 0$$

(7), (8)

The voltage across the series and intermediate capacitors Cs and Ca is expressed using (6) and (8).

$$V_{C_s} = \frac{2D}{D-1} V_{spk}$$

$$V_{C_a} = \left(\frac{1+D}{1-D}\right) V_{spk} \qquad (9), (10)$$

Additionally, using (7) and (9), the necessary voltage conversion ratio (Mv) of the proposed converter is determined.

$$\frac{V_{dc}}{V_{spk}} = \frac{3D+1}{1-D} = M_v \qquad (11)$$

Every switching cycle involves repeating the same set of actions. The main switching waveforms for these converter's components are displayed in Fig.6 during a switching cycle.

The output voltage (Vdc) of this enhanced SEPIC converter is measured and contrasted with the reference DC voltage (Vdc ref) in order to generate the necessary switching sequence for main switch S1 and auxiliary switch Sa. After this comparison, the error is treated using a PI (proportional integral) controller, which outputs the signal CVDC. The following equations describe the error and control signals at the sampling instant k.

$$V_{dce}(k) = V_{dcref}(k) - V_{dc}(k)$$

$$C_{Vdc}(k) = C_{Vdc}(k-1) + K_p\{V_{dce}(k) - V_{dce}(k-1)\} + K_i V_{dce}(k)$$

(12),(13)

Where Kp and Ki stand for the voltage PI controller's tuned settings. The control signal Cvdc is provided to the PWM generator, which creates the necessary pulse sequence for the upgraded SEPIC PFC converter by comparing it to a high-frequency carrier wave St in accordance with the following relation:

$$\text{If } S_t < C_{vdc} \text{ then } S_1 \text{ and } S_a \text{ is ON}$$

else, both OFF (14)

As a result of both switches being turned on simultaneously, controlling this converter is straightforward and simple to accomplish. To give the suggested converter intrinsic PFC features, a precisely regulated output is generated at the output during steady state and rapid transients in mains voltage.

2. Operation of Isolated Converter

In order to control the charging current during the CC and CV charging modes and to give the battery the necessary isolation, a flyback converter that was built in DCM was employed.

The following three modes are used to describe how the flyback converter works:

When switch Sf is switched on, mode I begins. As the input energy is stored at this moment, more current is flowing via the magnetising inductance. The output diode Df is biased in the opposite direction, and there is no energy transfer through the secondary winding. Through the output capacitor Cch, the battery receives the necessary charging current. The following is how you get the expression for peak current stress by switching Sf:

$$i_{sf} = i_{Lf} = \int_{t_1}^{t_2} V_{dc}\,dt + i_{Lf}(0) = \frac{V_{dc}}{L_f}(t_1 - t_2) + i_{Lf}(0) \quad (15)$$

where the magnetizing inductance current at instant t1 is represented by iLf(0). The formula for peak switch current is as follows:

$$i_{sf}(D_{ch}T_s) = \frac{V_{dc}D_{ch}}{L_f f_s} + i_{Lf}(0) \quad (16)$$

Where Ts (1/fs) is the isolated converter's switching interval, chosen in this section to be 20µs, and Dch stands for the converter duty cycle. The formula used to determine peak diode voltage is as follows:

$$V_{Dfm} = -\frac{V_{dc}}{N} + V_{ch} = -\frac{V_{ch}}{D_{ch}} \quad (17)$$

N stands for the HF transformer's transformation ratio, and Vch is the DC voltage that must be maintained at the charger output in order to retain the rated battery current. The primary winding voltage's polarity is reversed when the switch Sf is turned off during mode II. As the magnetizing inductance releases its energy to deliver the rated battery current, the rectifier diode at the secondary switches on at this precise moment. The expression for the magnetizing inductance current at this moment is,

$$i_{Lf} = \frac{1}{L_f}\int_{t_2}^{t_3}(-NV_{ch})dt + i_{Lf}(D_{ch}T_s)$$
$$= \frac{(-NV_{ch})}{L_f}(t_3 - t_2) + \frac{V_{dc}D_{ch}}{L_f f_s} + i_{Lf}(0) \quad (18)$$

where the magnetizing inductance current, iLf (DchTs), was measured at instant t2. Consequently, the following is how the diode current iDf is calculated:

$$i_{Df} = Ni_{Lf} \quad (19)$$

The expression for peak switch voltage is written as,

$$V_{Sfm} = V_{dc} + NV_{ch} = \frac{NV_{ch}}{D_{ch}} \quad (20)$$

DCM, which ends at time t3, is the name of this mode. The energy contained in the magnetising inductance, Lf, is totally used up in this mode. The rated battery load is currently supplied by the output capacitor Cch.

$$i_{Df} = i_{Sf} = 0 \quad (21)$$

B. Design of SEPIC PFC Converter based EV battery Charger

The upgraded SEPIC PFC converter and the isolated converter in DCM mode make up this charger's architecture. The upgraded SEPIC PFC converter is designed based on the given design expressions in [12].

4. RESULTS AND DISCUSSION

A. Bridgeless Cuk Converter Based EV Battery Charger

Performance of Charger at Steady State

The performance of an enhanced EV charger utilizing a BL Cuk converter was examined during steady state conditions, as illustrated in Figs. 7.1 - 7.2. Various parameters, including mains voltage, mains current, battery voltage (Vbatt), and battery current (Ibatt), were recorded during the constant current (CC) charging mode. From Fig. 7.1, it can be observed that the charger draws a unity power

factor (PF) current from the mains, which aligns in phase with the supply voltage. This confirms the improved power quality (PQ) performance of the charger, complying with the recommended PQ regulations.

Furthermore, Fig.7.1 demonstrates that the output voltage of the Bridgeless Cuk converter is precisely controlled at a constant 400V, which is necessary to supply power to the flyback converter at the output. The output of the flyback converter is effectively regulated at 53V, slightly higher than the battery voltage. This ensures that the battery consistently draws a current of 10A from the mains throughout the entire CC charging process, as indicated by the battery current.

In Fig.7.4, the voltage and current stress on the PFC switches S1 and S2 during their respective half cycles are depicted for the BL Cuk converter. The recorded switch current waveforms clearly indicate that the switch currents, Is1 and Is2, do not contribute to any circulating current flow during both the positive and negative half cycle operations. This observation validates that the proposed BL Cuk converter does not have any circulating current passing through the input inductors Li1 and Li2. This is due to the absence of interconnection between intermediate capacitors, as mentioned earlier in the topological discussion, which eliminates the formation of a circulating current loop. As a result, the charger experiences reduced circulating power loss, leading to an improvement in converter efficiency. In Fig 7.5, we can notice that the input current with THD of 46.43%

B. SEPIC PFC Based EV Battery Charger

Performance of Charger at Steady State

A. Performance of Improved Charger

The experimental findings regarding the enhanced efficiency of an electric vehicle (EV) charger utilizing a SEPIC converter are depicted in Figures 8.1 and 8.2. In Figure 8.1, the output voltage Vsepic of the SEPIC converter is carefully controlled and maintained at a constant value of 400V, as indicated in accordance with the converter's specifications.

The waveform diagrams presented in Figure 8.2 illustrate the voltage (Vbatt) and current (Ibatt) of the battery, correlating with the input voltage (Vs) and current (Is). It is evident from the graphs that the battery is undergoing a charging process with a consistent current flow of 10A. The enhanced power factor (PF) operation is distinguished by a synchronous current drawn from the power supply, resulting in an in-phase relationship between the supply current and voltage.

B. Performance of SEPIC Converter:

The steady-state performance of the high voltage gain operation of the SEPIC converter in discontinuous conduction mode (DCM) has been successfully validated. Figure 8.3 illustrates the voltage and current levels experienced by the main and auxiliary semiconductor devices during power factor (PF) correction. Upon closer examination of the switch voltage, it can be observed that switches endure a voltage stress of 600V. The increased voltage gain of the converter leads to a reduced duty cycle requirement for achieving the same DC-link voltage of 400V, resulting in lower switch voltage stress. Similarly, the voltage stress across the auxiliary diode Da can be observed in Figure 8.5.

The voltage and current levels observed in the main and auxiliary semiconductor devices, as well as the output inductor current (ILo) in DCM and input inductor currents (IL1, IL2) in CCM, as depicted in Figure 8.4, remain within justifiable limits. Notably, when examining the zoomed waveforms of the switches and diodes voltage, it becomes apparent that the converter exhibits inherent soft switching characteristics due to the selection of DCM operation. The peak current stress experienced by the output inductor reaches 2000A, which confirms the appropriate selection of the output inductance value. Additionally, Figure 8.5 provides a comprehensive illustration of the continuous voltage across the energy transfer capacitances (Cs and Ca) throughout one complete switching cycle. In Fig 8.6, we can notice that the input current with THD of 46.89%

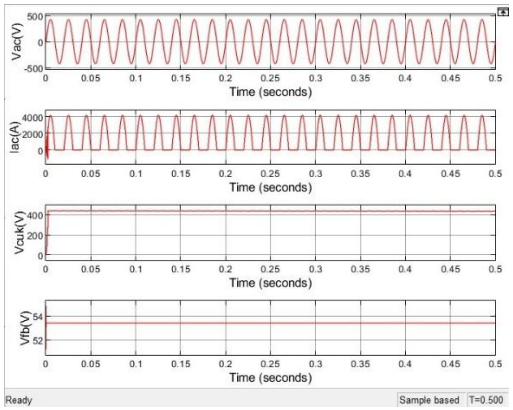

Figure 7.1: Source side quantities (Vac, Iac), DC link voltage of Bridgeless Cuk converter (Vcuk), flyback converter output characteristics (Vfb)

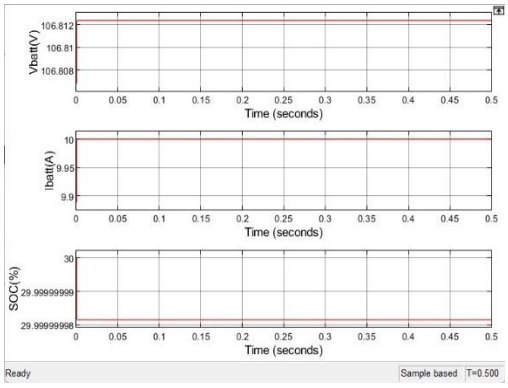

Figure 7.2: Battery side quantities (Vbatt, Ibatt, State Of Charge) of Bridgeless Cuk Converter Based EV Battery Charger

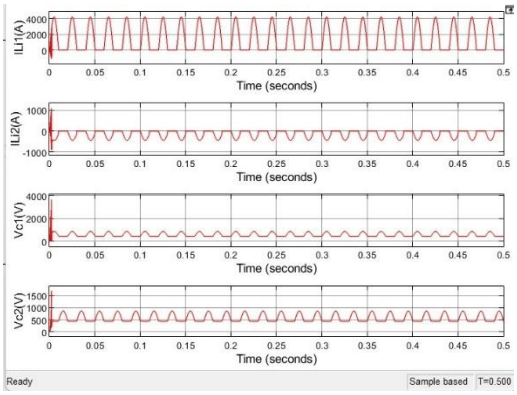

Figure 7.3: Inductor currents (ILi1, ILi2) and Capacitor voltages (Vc1, Vc2) of Bridgeless Cuk Converter Based EV Battery Charger in positive and negative half cycles respectively

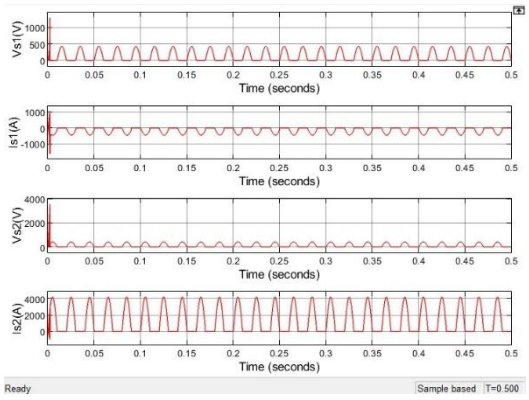

Figure 7.4: Switch voltages and currents waveforms (Vs1, Is1, Vs2, Is2) of switches S1 and S2 of Bridgeless Cuk Converter Based EV Battery Charger respectively

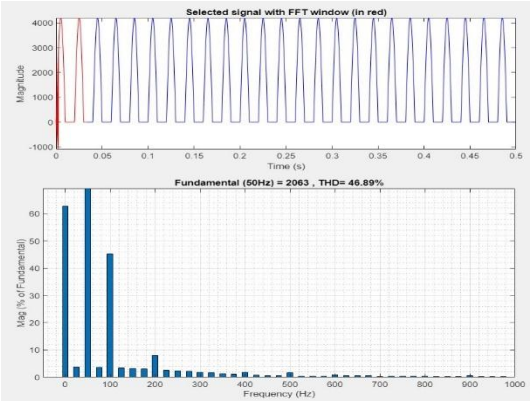

Figure 7.5: THD of input current of Bridgeless Cuk Converter Based EV Battery Charger

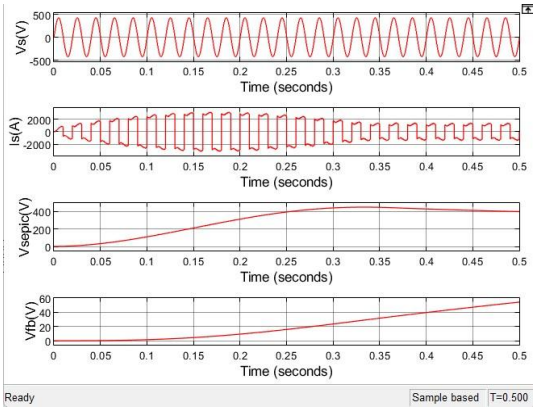

Figure 8.1: Source side quantities (Vs, Is) , DC link voltage of SEPIC PFC(Vsepic), Isolated converter output characteristics(Vfb)

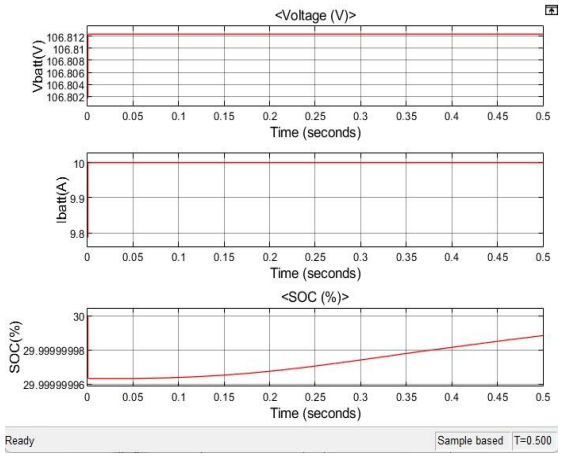

Figure 8.2: Battery side quantities(Vbatt, Ibatt, State Of Charge) of SEPIC PFC Converter Based EV Battery Charger

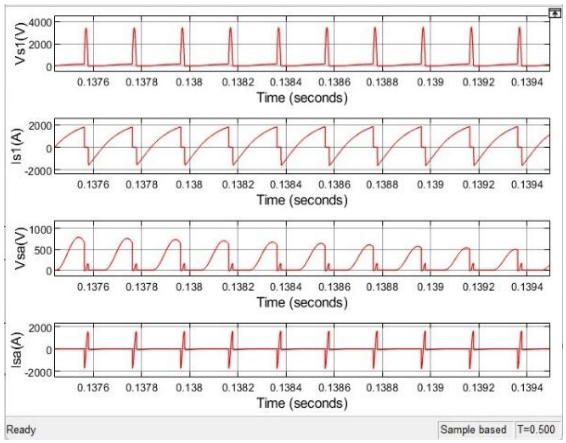

Figure 8.3: Switch voltages and currents waveforms(Vs1,Is1,Vsa,Isa) of switches S1 and Sa of SEPIC PFC Converter Based EV Battery Charger respectively

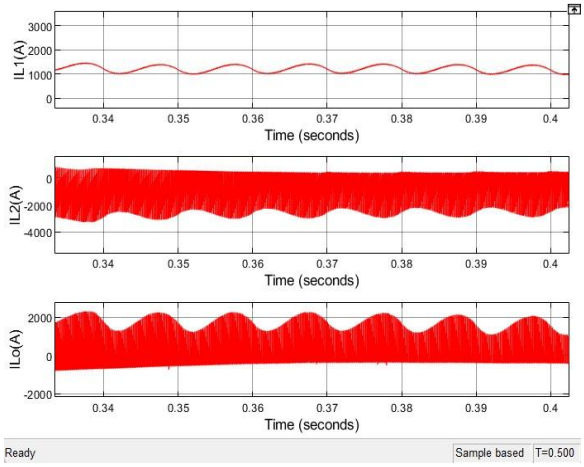

Figure 8.4: Inductor currents (IL1, IL2, ILo) of SEPIC PFC Converter Based EV Battery Charger

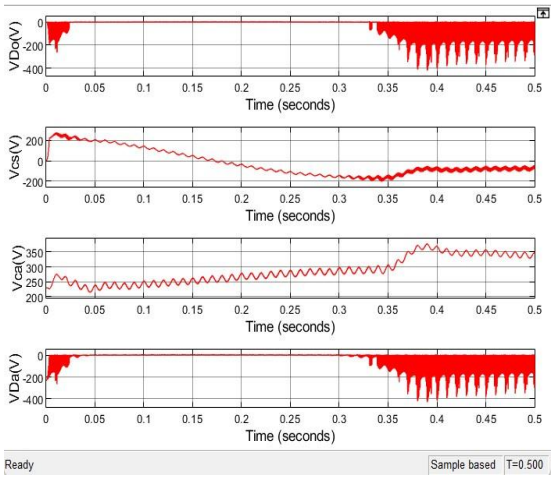

Figure 8.5: Switch voltage of output diode Do, voltage across the energy transfer capacitances Cs and Ca, Switch voltage of auxiliary diode Da of SEPIC PFC Converter Based EV Battery Charger respectively

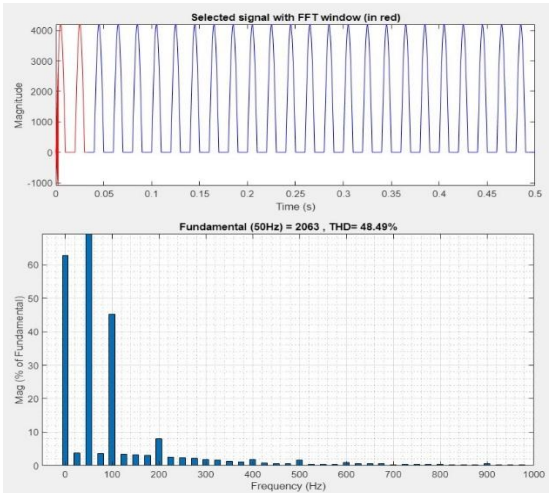

Figure 8.6 : THD of input current of SEPIC PFC Converter Based EV Battery Charger

5.CONCLUSION

Both the Bridgeless Cuk Converter with Flyback Converter and the SEPIC PFC Converter with Flyback Converter offer power quality improvement in EV chargers, but they also come with their own set of disadvantages.

Table 2. The key differences that are observed between Bridgeless Cuk Converter combined with a Flyback Converter and a SEPIC PFC combined with a Flyback Converter

Parameter	Bridgeless Cuk Converter + Flyback Converter	SEPIC PFC + Flyback Converter
Power Factor	Unity Power Factor (0.999)	Unity Power Factor (0.976)
Total Harmonic Distortion	Lower (46.89%)	High (48.49%)
Voltage Stress across Switches	Low(450V)	Moderate to High(600V)
Current Stress on Switches	Low(750A)	Moderate to High(1600A)
Voltage across Capacitors	850V	350V
Cost and Weight	Less	More
Complexity	High	Low

The Bridgeless Cuk Converter combination demonstrates several advantages, including a higher power factor of 0.999 compared to 0.976 for the SEPIC PFC combination. Moreover, the Bridgeless Cuk Converter combination exhibits lower total harmonic distortion (THD) at 46.89% compared to the higher THD of 48.49% for the SEPIC PFC combination i.e., the Bridgeless Cuk Converter combined with the Flyback Converter has approximately 3.3% lower THD compared to the SEPIC PFC combined with the Flyback Converter.

The Bridgeless Cuk Converter combination exhibits a lower voltage stress across switches of 450V compared to the moderate to high voltage stress of 600V in the SEPIC PFC combination. This indicates that the Bridgeless Cuk Converter combination imposes less strain on the switches, potentially leading to improved reliability and longevity.

Furthermore, the current stress on switches is lower in the Bridgeless Cuk Converter combination at 750A, whereas the SEPIC PFC combination experiences a higher current stress of 1600A. This highlights the Bridgeless Cuk Converter combination's ability to handle lower current levels, which can contribute to reduced losses and increased efficiency.

Regarding voltage across capacitors, the Bridgeless Cuk Converter combination operates at a higher voltage of 850V compared to the lower voltage of 350V in the SEPIC PFC combination. This higher voltage provides the Bridgeless Cuk Converter combination with greater energy storage capabilities and potential for improved performance.

Additionally, the Bridgeless Cuk Converter combination achieves higher efficiency, while being less costly and lighter. However, it is worth noting that the Bridgeless Cuk Converter combination is more complex in terms of design. Overall, the Bridgeless Cuk Converter combined with the Flyback Converter outperforms the SEPIC PFC combined with the Flyback Converter in terms of power factor, THD, stress levels, efficiency, cost, and weight.

6. REFERENCES

[1] C. Chan and K. Chau, "Power electronics challenges in electric vehicles," in Proc. IEEE IECON'93., pp. 701–706.

[2] Limits for Harmonics Current Emissions (Equipment current ≤ 16A per Phase), International standards IEC 61000-3-2, 2000.

[3] Bhim Singh, Brij N. Singh, Ambarish Chandra, Kamal Al-Haddad, Ashish Pandey, and Dwarka P. Kothari. "A review of single-phase improved power quality AC-DC converters," IEEE Transactions Industrial Electronics, vol.50, no. 5, pp.962-981, July 2003.

[4] L. Huber, Y. Jang, and M. Jovanovic, "Performance evaluation of bridgeless PFC boost rectifiers," IEEE Transactions Power Electronics, vol. 23, no. 3, pp. 1381–1390, May 2008.

[5] B. Zhao, A. Abramovitz and K. Smedley, "Family of bridgeless buck-boost PFC rectifiers," IEEE Transactions Power Electronics, vol. 30, no. 12, pp. 6524-6527, Dec. 2015.

[6] D. S. L. Simonetti, J. Sebastian, F. S. dos Reis and J. Uceda, "Design criteria for SEPIC and Cuk converters as power factor preregulators in discontinuous conduction mode" in Proc. International Conference on Industrial Electronics, Control, Instrumentation, and Automation, 1992, pp. 283-288 vol.1.

[7] A. A. Fardoun, E. H. Ismail, A. J. Sabzali and M. A. Al-Saffar, "New Efficient Bridgeless Cuk Rectifiers for PFC Applications," IEEE Transactions on Power Electronics, vol. 27, no. 7, pp. 3292- 3301, July 2012.

[8] T. J. Liang, K. H. Chen and J. F. Chen, "Primary Side Control For Flyback Converter Operating in DCM and CCM," IEEE Transactions Power Electronics, vol. 33, no. 4, pp. 3604-3612, April 2018.

[9] K. Yao, X. Ruan, X. Mao and Z. Ye, "Variable-Duty-Cycle Control to Achieve High Input Power Factor for DCM Boost PFC Converter," IEEE Transactions Industrial Electronics, vol. 58, no. 5, pp. 1856-1865, May 2011.

[10] SAE Electric Vehicle and Plug-in Hybrid Electric Vehicle Conductive Charge Coupler, SAE Std. J1772, 2010.

[11] Kushwaha, R., & Singh, B. (2018). A Power Quality Improved EV Charger with Bridgeless Cuk Converter.2018 IEEE International Conference on Power Electronics, Drives and Energy Systems (PEDES).

[12] Kushwaha, R., & Singh, B. (2019). An Improved SEPIC PFC Converter for Electric Vehicle Battery Charger.2019 IEEE Industry Applications Society Annual Meeting.